Original

PAPER

Polyglycerol-based polymer network films for potential biomedical applications

Duygu Ekinci, Adam L. Sisson and Andreas Lendlein*

Synthetic polymeric materials are established as being central to many modern approaches to medical treatments such as biomaterial induced tissue regeneration or drug eluting implants. Cytocompatible, antifouling materials, based on hydrophilic polymers such as poly(ethylene glycol), have been widely studied as a 'blank canvas' substrate; it is possible to apply various bioactive ligands to elicit specific tissue and cell responses. In recent years, branched polyglycerols have gained attention as a viable alternative to PEG as a protein-resistance providing chemical moiety. To this end we have embarked on the preparation of bulk polyglycerol-based films, which are readily synthesized from abundant starting materials, with the aim of evaluating their as yet undiscovered potential as macroscopic biomaterials. Herein we report syntheses, as well as mechanical, and rheological properties of a series of polyglycerol-based polymer networks. Polymeric films produced are highly crosslinked, have high thermal stability, and are flexible with thermal glass transition temperatures below body temperature.

Introduction

In the last couple of decades an intense interest in the use of polymeric networks for biomaterial applications has developed. In particular, polymeric hydrogels are explored in various aspects of regenerative medicine.[1,2] The central paradigm developed from an understanding that synthetic matrices could in many ways mimic natural extracellular matrices, which are essential to regulate cell and tissue behaviors in biological systems.[3] Numerous functions such as cellular attachment, structural and rheological parameters, degradability, and solute diffusion could in principle be rationally controlled during synthesis with the overall aim to develop a knowledge-based approach to biomaterial design. Various hydrophilic synthetic polymers and copolymer architectures are currently investigated with poly(ethylene glycols) (PEG), polyvinyl alcohols (PVA) and poly(hydroxyethyl methacrylates) (PHEMA) being substantially the most widely employed in highly branched or network polymers. Neutral, hydrophilic, polyether/polyols are regarded to confer good biocompatibility with protein resistance and thus can provide a benign substrate for biomaterial applications, as has been utilized with PEG in many areas of polymer therapeutics.[4] Such polymeric structures bear semblance to abundant polysaccharides in ECM such as hyaluronan and heparin. Currently, the fundamental processes occurring between polymeric materials and biological substrates determine cell adhesion, influence cell differentiation and metabolism, constitute an area of vigorous study. Protein resistant substrates make excellent base scaffolds for controlling cell and tissue specific material interactions as they can be surface functionalized with specific moieties that drive selective interactions and give biomimetic functions.[5] It is of paramount importance to limit the amount of surface protein adsorption to such materials, as in physiological milieu, biofilms form extremely rapidly on unsuitable substrates thus removing any control over surface properties. To this end PEG networks receive much interest with various bioactive ligands being attached to the otherwise highly protein resistant surface.[6]

Although PEG has shown excellent promise in biomaterial applications due to the inherent protein resistance, there are some downsides with regards to synthetic utility. PEG is essentially a linear polymer, so extra synthetic steps are required to incorporate it into a branched polymer network. Although circumventing these limitations is somewhat trivial by copolymerization or by employing starshaped PEGs originating from multivalent initiators, there is still the limitation that as a linear polymer the density of functionalizable terminal groups is steeply inversely proportional to its molecular weight. An alternative biocompatible polyether polyol,[7] with a hyperbranched structure, can be considered in hyperbranched polyglycerol (hPG),[8] which in recent years attracts interest for the range of applications traditionally seen for PEG. The development of hPG chemistry is further driven as the raw materials may be considered sourced from renewable plant oil stocks as glycerol is a byproduct of biodiesel production.[9] Polyglycerols have been prepared on all dimensional scales from dendritic polymers, through to emulsion templated nanogels,[10] microfluidic

Center for Biomaterial Development, Institute of Polymer Research and Berlin Brandenburg Center for Regenerative Therapies, Helmholtz-Zentrum Geesthacht, Kantstr. 55, D-14513 Teltow, Germany. E-mail: andreas.lendlein@hzg.de; Fax: +49 (0)3328 352-452; Tel: +49 (0)3328 352-450

templated microparticles,[11] electrospun fibres,[12] and macroscopic hydrogels. The aforementioned macrogels have been shown to be able to encapsulate stem cells as an experimental artificial niche material.[13] Self-assembled monolayers containing linear polyglycerol or hPG dendrons have been shown to have strong antifouling properties analogous to PEG; smart surfaces have been reported with polyglycerol based monolayers which could switch from a bioinert to a strongly cell adhesive state by utilizing thermal transitions influencing the swelling state of such monolayers.[14]

Routes to prepare dendritic hPG were first established by anionic ring-opening multi-branching polymerization of latent AB$_2$ monomer glycidol (3-hydroxypropylene oxide).[15,16] In the anionic case molecular weights up to around 10 000 g mol^{-1} are achievable with low polydispersity, although suspension polymerization has resulted in particles up to 1 000 000 g mol^{-1}.[17] A method to prepare bulk hydrogels based on hPG segments has been developed by photocrosslinking of methacrylate functionalized dendritic (ca. 2000 g mol^{-1}) prepolymers; a process which is also amenable to soft lithography techniques to give defined microscale materials.[18,19] Cationic ring-opening polymerizations (ROP) of glycidol also proved to be effective in preparing comparable hPG dendritic polymers with a range of Lewis and Brønsted acids.[20,21] In the previous research we have investigated the cationic ROP of glycerol glycidyl ether (GGE) under miniemulsion conditions resulting in polyglycerol-based nanogels;[22] this was recently extended to incorporate a range of other multivalent glycidyl ethers.[23] Cationic photopolymerization of various di-, tri- and tetraol based glycidyl ethers has been investigated for kinetic studies with elastomeric bulk polymer network films resulting.[24,25]

With the aim of preparing a material scaffold, which can be employed in studying/manipulating cell and tissue specific interactions, we have chosen to investigate bulk polyglycerol-based polymer network (PGBN) films. Despite the apparent benefits of such a polyglycerol-based polymer network architecture, these materials have not appeared in the literature for biomaterial applications whereas much attention has been devoted to PEG and other hydrophilic polymer based systems. It is highly reasonable to expect PGBN films to have antifouling properties with a chemical structure lending itself to surface hydration.[26] Due to this we anticipate these films to be a bioinert substrate, on which bioactive ligands may be attached, ultimately controlling cell–material interactions.[27] As a direct consequence, sophisticated cell culture systems are envisaged, which can be tailored towards eliciting various effects such as:[28] preferential adhesion and proliferation/matrix-deposition of specific cell types; controlled spatial organization of adherent cells through surface patterning; or as substrates to control differentiation and behavior of adhered multipotent stem cells. Furthermore, such polymer networks could have applications in regenerative medicine as otherwise inert implant materials, which can be modified to release bioactive substances in a controlled fashion, control biofilm deposition to provide hemocompatibility, or promote tissue growth in a defined manner (including 3-dimensional scaffolds). A high degree of control over the bulk material properties are essential for such applications as the cellular response to physical and chemical cues from the extra cellular matrix is of critical importance to tissue development.[29]

In many cases, polymeric substrates must be treated in order to modify hydrophilicity/wetting and other properties that lead to antifouling,[30] whereas PGBN films can be prepared in a facile manner with an inherently polyether/polyol polyvalent, hydrophilic surface. A major advantage of branched polyglycerol-based systems over PEG is that the number of alcohol terminal groups available for derivatization is less limited by increasing chain lengths and branching points. Many recent efforts are directed towards attaching various bioresponsive ligands to surfaces to give smart materials, and an easily functionalizable surface greatly increases the potential to easily investigate a wider range of ligands.[31,32] Here we report the preparation of polyglycerol-based bulk polymer elastomeric films and extensive rheological and mechanical analyses of the networks. Multifunctional glycerol based glycidyl ethers were photopolymerized as homopolymer networks or as copolymers with various monoglycidyl ethers to control factors such as crosslink density, mechanical properties, and thermal transition temperatures.

Experimental section

Materials

Glycerol glycidyl ether was purchased from Raschig GmbH (Ludwigshafen, Germany) and distilled under reduced pressure prior to use. Methyl glycidyl ether, ethyl glycidyl ether, isopropyl glycidyl ether, n-butyl glycidyl ether (ABCR, Karlsruhe, Germany) and photoinitiator diphenyliodonium hexafluorophosphate (Sigma Aldrich, Hannover, Germany) were used without further purification. The structures of all monomers and the photoinitiator are shown in Fig. 1 together with their abbreviations.

Synthesis and network formation

Synthesis of PGBN films is a one-step procedure, which is based on photopolymerization of the initial glycidyl ether monomer mixture, in which the photoinitiator is dissolved. The initial monomer mixture is composed of either the GGE crosslinker
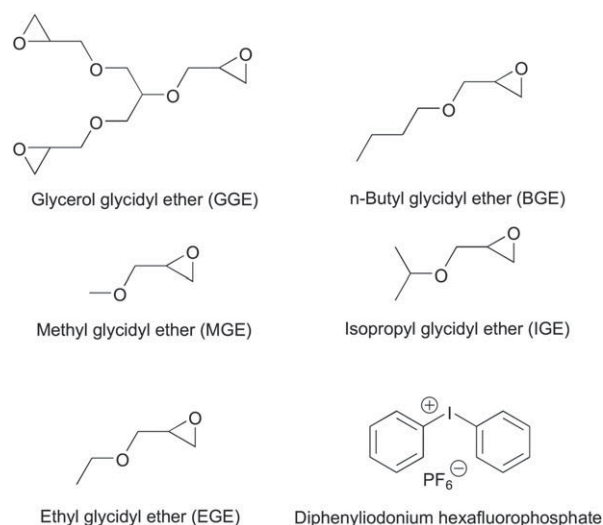

Fig. 1 Structure of monomers and the photoinitiator.

This journal is © The Royal Society of Chemistry 2012

J. Mater. Chem., 2012, 22, 21100–21109 | 21101

itself or the selected alkyl glycidyl ether and the crosslinker, where the alkyl glycidyl ethers act as the chain extension segments (Table 1). The initial mixture is poured into a mould formed by two silanized glass slides (25 mm × 75 mm), where a Teflon frame of 0.5 mm thickness is placed in between as the spacer to determine the thickness of the final product. Photo-polymerization is performed with a UVEX model SCU-110 mercury lamp, which is placed at a distance of 5 cm from glass slides. The light intensity at this distance was measured at 155 mW cm^{-2} using a PLUS-USB Energy & Power Meter equipped with a Sensor A-40-D25-HCB (Laserpoint, Milan, Italy). The mercury lamp emits the main UV peak at 365 nm wavelength, which is above that at which the silanized glass plates showed any significant absorbance. The reaction of this initial mixture leads to a translucent film formation; the film products were left at dark for postcuring for 4 days.

Cross-sections (10 mm × 20 mm) were taken from the cured translucent film samples and immersed in ethanol overnight for swelling and removal of the unreacted components. The swollen films were then weighed and dried at 50 °C in a high vacuum for one week until the weight reaches a constant value. For each crosslinked polymer network, gel content, degree of swelling, crosslink density, and number average molecular weight between the crosslinks (*i.e.* network chain segment) are determined.

Gel content G and degree of swelling Q are calculated according to eqn (1) and (2).

$$G = \frac{m_d}{m_{iso}} \times 100\% \qquad (1)$$

$$Q = 1 + \rho_p \left[\frac{m_s}{m_d \times \rho_s} - \frac{1}{\rho_s} \right] \qquad (2)$$

where m_{iso}, m_d and m_s are the weights of the crude, swollen and dry film, ρ_p and ρ_s are the densities of the polymer and the swelling agent respectively. Crosslink density and number average molecular weight between crosslinks are calculated by using the modified Flory–Rehner equation (eqn (3–6).[33]

Crosslink density:

$$\gamma = -\frac{\left[V_r + \chi V_r^2 + \ln(1 - V_r) \right]}{d_r V_0 \left[V_r^{1/3} - \frac{V_r}{2} \right]} \qquad (3)$$

$$\theta = \frac{m_s - m_{iso}}{m_s} \times \frac{\rho_p}{\rho_s} \qquad (4)$$

$$V_r = \left[\frac{1}{1 + \theta} \right] \qquad (5)$$

Number average molecular weight between crosslinks:

$$\overline{M_c} = \frac{1}{\gamma} \qquad (6)$$

where θ is the swelling coefficient, V_r the volume fraction of the polymer, d_r the density of polymer, V_0 the molar volume of the swelling agent and χ the polymer–solvent interaction parameter, also called the Flory–Huggins interaction parameter. The Flory–Huggins theory, modified by Blanks and Prausnitz (1964), allows establishing a relation between the Flory–Huggins parameter and the solubility parameters of the polymer δ_p and solvents δ_s (eqn (7)).[32] The solubility parameter of a polymer is defined as a characteristic of a polymer used in predicting the solubility of that polymer in a given solvent. For polymers, it is usually taken to be the value of the solubility parameter of the solvent producing the solution with maximum swelling of a network of the polymer.

$$\chi = \chi_s + \frac{V_1}{RT}(\delta_p - \delta_s)^2 \qquad (7)$$

where V_1 is the molar volume of the solvent and χ_s the entropic contribution to χ. The value of χ_s is typically kept constant and equal to 0.34.[34] Therefore, the polymer–solvent interaction parameter takes the value of 0.34 for $\delta_p = \delta_s$.

Rheology analysis

Rheological analysis of PGBN films was performed on a Physica MCR 501 rheometer (Anton Paar GmbH) equipped with an external UV-light source (OmniCure UV LED spot curing system) having a 365 nm UV LED head with 9500 mW cm^{-2} irradiance. Both the shear conditions and the measuring temperature are kept constant. Starting reaction mixtures are placed on the glass plate through which UV-light irradiation passes from the source below. The gap between the glass plate and the metal plate of the measuring system is set at a distance of 0.3 mm.

FTIR spectroscopic analysis

FT-IR transmission spectra of PGBN film samples are obtained using a Tensor 27 FT-IR Spectrometer (Bruker) with a standard DLaTGS-Detector.

Thermal analysis

Thermal properties of the polymer networks were investigated by TGA, DSC, and DMTA.

Thermal gravimetric analysis (TGA) of the samples was performed on a TG 209 apparatus (Netzsch). The film samples were heated from 25 °C to 400 °C at a heating rate of 10 K min^{-1}.

Table 1 Chemical composition of PGBNs studied

Monomer	Notation	Monomer		Crosslinker[a]	
		Wt%	Mol%	Wt%	Mol%
None	G_{100}	0	0	100	100
MGE	$G_{80}M_{20}$	20	43	80	57
MGE	$G_{60}M_{40}$	40	66	60	34
MGE	$G_{40}M_{60}$	60	82	40	18
EGE	$G_{80}E_{20}$	20	39	80	61
EGE	$G_{60}E_{40}$	40	63	60	37
EGE	$G_{40}E_{60}$	60	79	40	21
IGE	$G_{80}I_{20}$	20	36	80	64
IGE	$G_{60}I_{40}$	40	60	60	40
IGE	$G_{40}I_{60}$	60	77	40	23
BGE	$G_{80}B_{20}$	20	33	80	67
BGE	$G_{60}B_{40}$	40	57	60	43
BGE	$G_{40}B_{60}$	60	75	40	25

[a] GGE as the crosslinker, initiator concentration was kept at 2.0 wt% with respect to the initial mixture amount.

Differential scanning calorimetry (*DSC*) was performed on a DSC 204 apparatus (Netzsch). The film samples were heated from 25 to 250 °C at a heating rate of 10 K min^{-1}, kept at this temperature for 2 minutes and cooled down to −100 °C at 10 K min^{-1} with a nitrogen purge and kept for 2 minutes at that temperature. Thermal properties were determined from the second heating run at 10 K min^{-1}.

Dynamic mechanical analysis at varied temperature (*DMTA*) was performed on an EPLEXOR QC 25 (GABO QUAL-IMETER Testanlagen GmbH) equipped with a 25 N load cell, at a frequency of 10 Hz and a heating rate of 2 K min^{-1} in a temperature range between −50 °C and +100 °C.

Mechanical analysis

Tensile properties of PGBN films were determined on a Zwick tensile tester (2.5N1S, Zwick GmbH & Co, Ulm, Germany) equipped with a 50 N load cell at an elongation rate of 2 mm min^{-1}. Sample dimensions were 3 mm × 10 mm with a thickness of about 0.3 mm.

Results and discussion

Network preparation and characterization

Translucent, PGBN films were prepared *via* crosslinking of various glycidyl ethers (Fig. 1 and Scheme 1), initiated by irradiation with UV-light in a cationic ring-opening polymerization

process. Diaryliodonium salts were used as photoinitiators, being among the reagents of choice for most commercial applications involving UV induced cationic photopolymerizations.[35] Subsequent to the irradiation of the monomer-initiator mixture, photolysis of the photoinitiator takes place forming a superacid.[36] Polymerization occurs *via* the typical steps for cationic ring-opening, however the kinetics of reaction are unusual and show strong tendencies towards frontal polymerization. During propagation, the acid-complexed, cationic epoxide intermediate is stabilized by the neighboring glycidyl ether (Scheme 1B), which causes reactions to proceed sluggishly until the exothermic reaction becomes autoaccelerated above a thermal threshold.[24] Theoretically the resulting carbocation can continue to propagate until all epoxide rings open, however steric and mobility restrictions make this unlikely. A carbocation at any stage can be terminated by the presence of a nucleophilic impurity such as water.[37] The resultant polymer would be a densely crosslinked network structurally related to dendritic hPG polymers formed by related methods.[20] The first step in the reaction involving acid generation is the only step that is light-driven. The remaining steps are dark steps, which proceed under the driving force of the relief of epoxy ring strain. In such polymerizations, postcuring is a crucial step, which means a long-lasting reaction after UV-irradiation, with propagation proceeding in the absence of further UV initiation.[25]

The ring-opening reaction could be monitored by FTIR spectroscopy. The reduction of the peaks at 3056, 2998, 907, 839
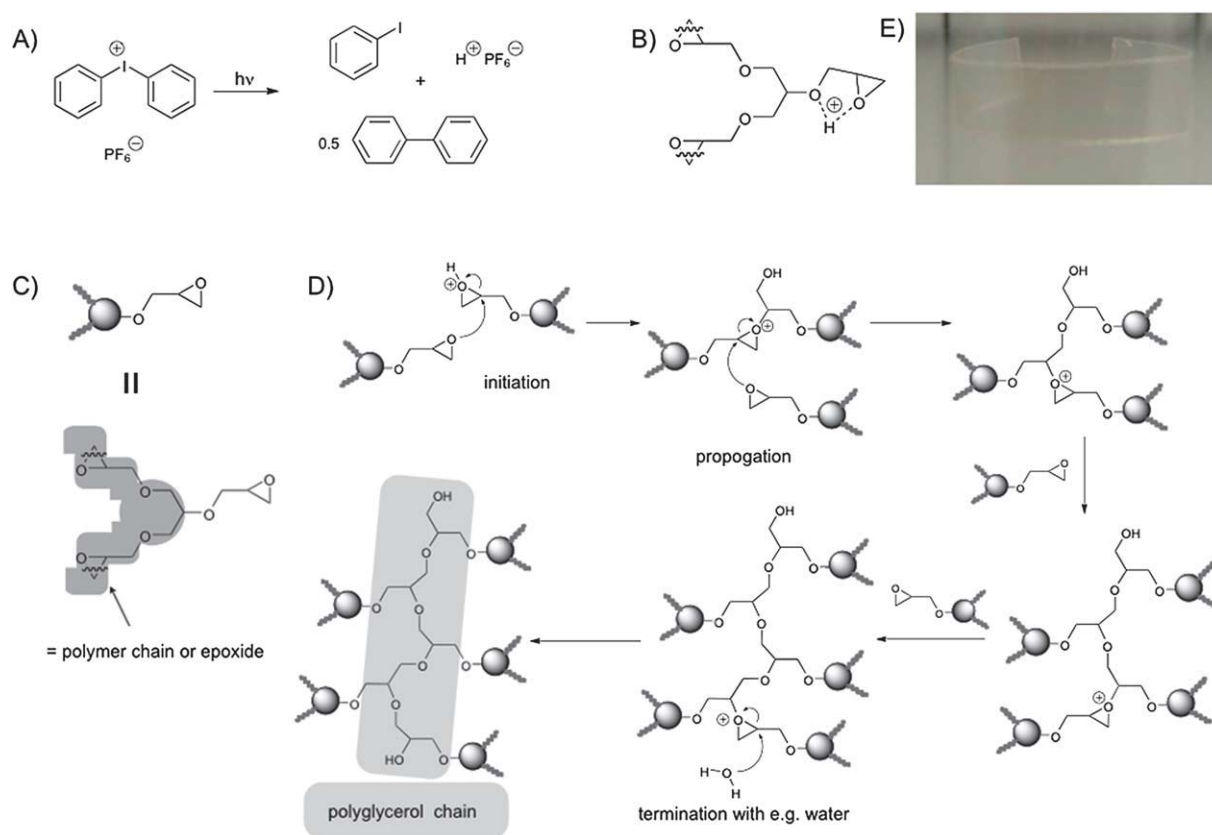
Scheme 1 Synthesis of UV-crosslinked PGBNs: (A) photolysis of the photoinitiator diphenyl hexafluorophosphate, (B) structure of the crosslinker GGE showing protonated mode, (C and D) exemplary reaction for PGBN formation by the monomer GGE and (E) film product placed within a glass sample tube to show the high degree of translucency.
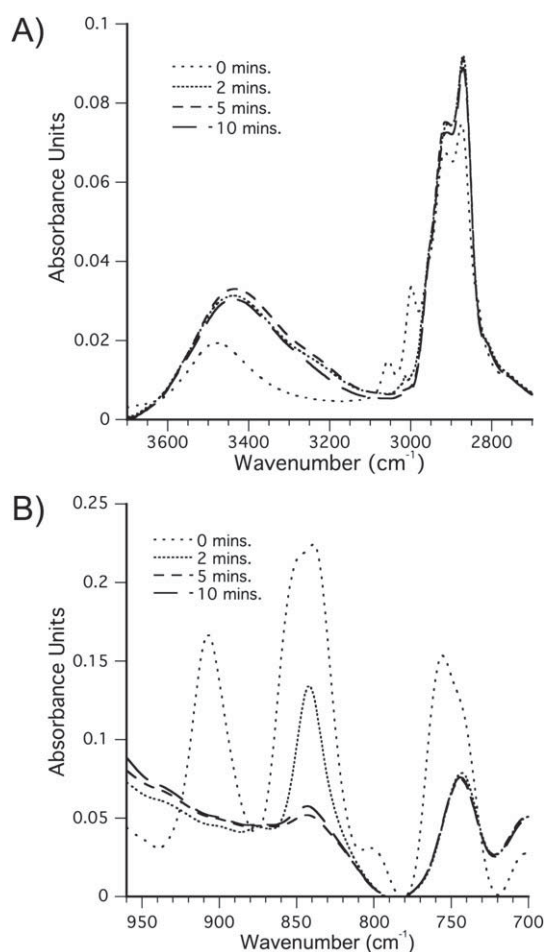
Fig. 2 Exemplary FT-IR spectra of a PGBN film showing decrease of the epoxy ring absorption at 3056, 2998, 907, 839 and 756 cm^{-1} depending on irradiation time intervals of 0, 2, 5 and 10 min.

and 756 wavenumbers, which are attributed to epoxy vibrational frequencies, is apparent as indicative of the ongoing ring-opening reaction; the literature states that peaks at 3056 and 2998 are particularly characteristic of oxirane compared to acyclic ethers (Fig. 2).[38] The broad absorbance from 3600 to 3300 cm^{-1} is related to the hydrogen-bonded OH groups. At 3432 cm^{-1} hydroxyl groups are formed by the acid-catalyzed epoxy ring-

opening reaction. High conversions are observed with no significant oxirane peaks remaining in the prepared films.

To investigate the network properties, swelling experiments were performed in ethanol. For each PGBN, the gel content is high (min. 97%) indicating high conversion. Gel content (G), degree of swelling (Q), crosslink density (γ), and the network chain segment length (number average molecular weight between crosslinks; $\overline{M}_n$) were calculated from swelling data according to the Flory–Rehner equations stated in the Experimental section. The compositions of copolymers employed had a significant influence on these parameters shown in Table 2. The crosslink densities and network chain segment lengths calculated are important parameters for network polymer characterization and are used as a basis to rationalize thermomechanical properties in the following section. To define the network chain segment length, Scheme 2 illustrates the influence of incorporation of monoglycidyl ethers (as distinct from the crosslinker GGE) on the copolymer systems. As propagation involving a mono-glycidyl ether results in a linear unit, the network chain segment length can be interpreted as the average molecular weight between GGE branching network points in the final copolymer.

As expected, incorporation of monomeric glycidyl ethers into the reaction mixture resulted in increased network chain segment lengths and proportional changes in related network parameters such as degree of swelling. It can be seen in Fig. 3A that the degree of swelling is directly proportional to the network chain segment length, as would be expected of a polymer network. This behavior can be directly correlated to the copolymer ratio as shown in Fig. 3B, where it is clear that $\overline{M}_n$ is strongly correlated to the amount of GGE incorporated into the polymer on a molar basis. Such analysis clearly indicates that the density of network points is strongly dependent on the mole fraction of crosslinker in the starting mixtures. Although higher values of $\overline{M}_n$ clearly allow more swelling, no profound significance on the nature of glycidyl sidechains of copolymers is observed when data are compared on a sidechain basis. The degree of swelling appears to be dependent primarily on the network chain segment length as may be expected for network polymers. This is a trend also reflected in the mechanical properties described below. All of the tested networks are densely crosslinked with low $\overline{M}_n$ values, as would be expected for a highly branched polymer network. Although it must be noted that these $\overline{M}_n$ values are relative approximations based upon the Flory–Huggins theory, they

Table 2 Chemical composition, degree of swelling (Q), gel content (G), density (ρ), crosslink density (γ), and network chain segment length ($\overline{M}_n$) of the PGBNs studied

Monomer/crosslinker composition	Q [V·V^{-1}]	G [%]	ρ [g cm^{-3}]	γ [mol cm^{-3}]10^3	$\overline{M}_n$ [g mol^{-1}]
G$_{100}$	1.13	99	1.43	28.2 ± 1	35.7 ± 7.8
G$_{80}$M$_{20}$	1.27	98	1.39	15.3 ± 1	65.0 ± 4.1
G$_{60}$M$_{40}$	1.35	98	1.22	14.2 ± 1	70.2 ± 7.1
G$_{40}$M$_{60}$	1.42	97	1.17	11.3 ± 0.1	79.1 ± 2.7
G$_{80}$E$_{20}$	1.27	96	1.12	21.9 ± 1	45.5 ± 3.8
G$_{60}$E$_{40}$	1.45	95	1.07	13.3 ± 0.1	74.9 ± 0.4
G$_{40}$E$_{60}$	1.51	97	1.01	12.9 ± 0.1	78.0 ± 0.1
G$_{80}$I$_{20}$	1.28	95	1.20	19.9 ± 5.3	50.2 ± 1.4
G$_{60}$I$_{40}$	1.43	90	1.17	14.9 ± 0.1	66.7 ± 3.8
G$_{40}$I$_{60}$	1.58	94	1.03	13.0 ± 0.4	76.7 ± 2.1
G$_{80}$B$_{20}$	1.26	97	1.30	17.2 ± 0.1	58.1 ± 6.3
G$_{60}$B$_{40}$	1.35	97	1.09	16.9 ± 0.5	58.8 ± 1.8
G$_{40}$B$_{60}$	1.65	92	1.08	11.8 ± 1.3	84.4 ± 10
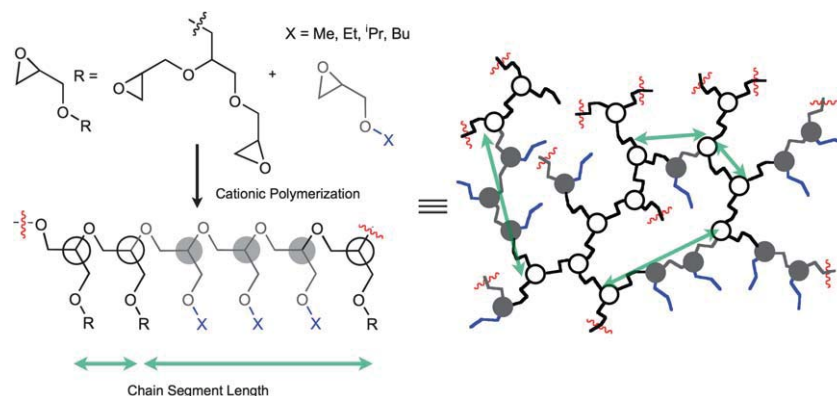
Scheme 2 Defined components of polyglycerol-based copolymer networks derived from glycerol glycidyl ether (R) and monoglycidyl ethers (X), and representation of a typical network structure with branching points (hollow circles), linear chain extending repeats (grey circles) and glycidyl ether sidechains (blue).

can be directly compared within this dataset, and show a clear trend based on the ratio of crosslinker to monoglycidyl ether content.
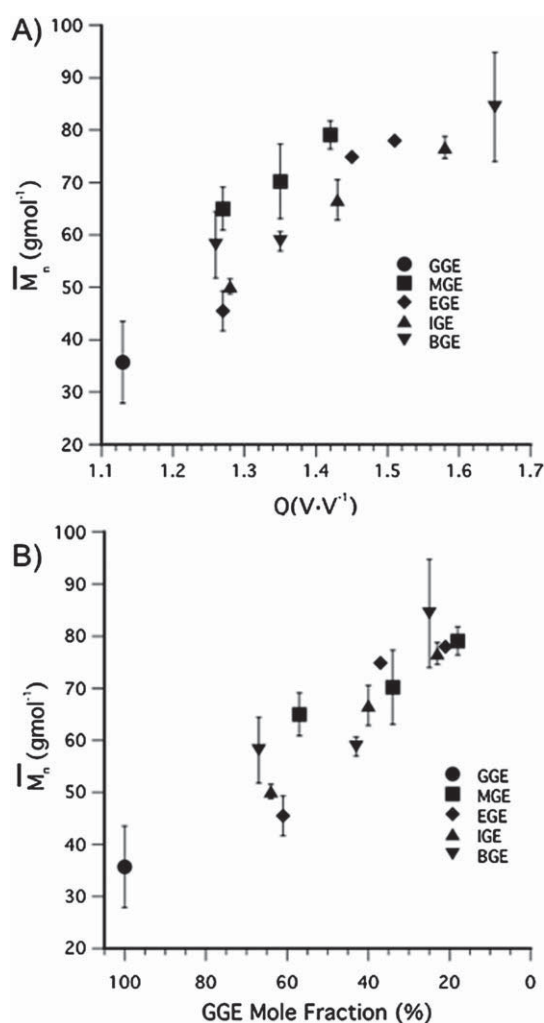
Reaction kinetics during crosslinking were investigated by rheological analysis. Each sample was irradiated by UV light until the ignition period was complete and network formation observed. Oscillatory tests were conducted to allow carrying out the measurement without any internal destruction to the sample during the curing process. Thus it was possible to examine the time dependent formation of a chemical network during the measurement. Initially, G'' (loss modulus) $> G'$ (storage modulus), characteristic of the viscous fluid reactants. Upon irradiation a delay period is observed, followed by a rapid increase in both moduli and an eventual inversion to show characteristics of a solid material where $G' > G''$. The gel time (t_{GT}) is measured at the intersection where $G' = G''$ or alternatively cited as tan $\delta = G''/G' = 1$, and signifies the onset of the hardening process in cured thermoset networks. Fig. 4 shows typical changes in rheological parameters during the polymerization process, and is indicative of an autocatalytic process where the rapid onset of gelation is observed after a delay period.

Analysis of gel time periods for the copolymers with different monoglycidyl ethers is complicated due to being dependent on

Fig. 3 Structure–property relationship between: (A) degree of swelling (Q) and network chain segment length ($\overline{M}_n$); and (B) mole fraction of crosslinker GGE and resultant $\overline{M}_n$; of PGBNs studied.
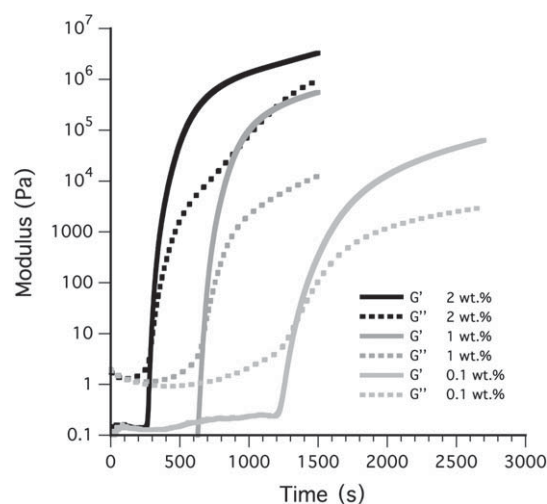

Fig. 4 Evolution of rheological storage and loss moduli (G' and G'' respectively) during the polymerization and hardening of GGE with varying initiator amounts of 2.0, 1.0, and 0.1 wt%.

Table 3 Chemical composition influence on gelation time periods (t_{GT}) obtained from rheology analysis for UV-cured PGBN films. Initiator concentration was kept at 2.0 wt% with respect to the initial mixture amount; reactions performed at a constant temperature of 50 °C, unless otherwise stated

Series	t_{GT} [s]
G_{100} (50 °C)	135
$G_{80}M_{20}$	216
$G_{60}M_{40}$	246
$G_{40}M_{60}$	249
$G_{80}E_{20}$	381
$G_{60}E_{40}$	435
$G_{40}E_{60}$	446
$G_{80}I_{20}$	387
$G_{60}I_{40}$	378
$G_{40}I_{60}$	366
$G_{80}B_{20}$	350
$G_{60}B_{40}$	383
$G_{40}B_{60}$	408
G_{100} (20 °C)	295[a,b]
G_{100} (20 °C)	640[a,c]
G_{100} (20 °C)	1310[a,d]

[a] Temperature maintained at 20 °C. [b] Initiator concentrations of 2.0 wt% (see Fig. 4). [c] Initiator concentrations of 1.0 wt% (see Fig. 4). [d] Initiator concentrations of 0.1 wt% (see Fig. 4).

complex thermodynamic and steric parameters. In general the onset of gelation was hindered by the addition of monomeric glycidyl ether chain extenders, as may be expected as the cross-link density is decreased (Table 3). As clear trends in physical, thermal and mechanical analyses have been observed for the studied films, this piece of evidence points towards a homogeneous network where the reactivities of crosslinker epoxides and monomer epoxides are sufficiently comparable to not form segregated phases under the reactant ratios employed. A possible exception could be the case when using IGE as a chain extender. Analysis of gel times shows a reverse trend where increasing the IGE content leads to a faster onset of gelation. Due to the secondary isopropyl chain in the ether side group, IGE has enhanced reactivity over the other alkyl glycidyl ethers used due to steric shielding of the glycidyl ether oxygen moiety. It is well established that the proximity of the glycidyl ether oxygen hinders cationic ring-opening due to competition of Lewis acid binding to the epoxide in such systems.[39] Although translucent films with comparable bulk mechanical properties to the other systems were prepared when IGE was employed, sensitive dynamic mechanical thermal analyses outlined below could indicate some heterophase separation for the case of IGE containing films. In such cases, highly crosslinked polyGGE rich regions may coexist with polyIGE rich long linear chains or form semi-interpenetrating polymer network regions.[40]

Thermal and mechanical properties of polyglycerol-based polymer networks

Thermal and mechanical properties of the PG networks were determined by TGA, DSC and DMTA. Thermal decomposition was analyzed by TGA for polymer networks. The general trend of weight loss is around 1 wt% up to 100 °C, which is possibly due to the loss of water. The network composed of only GGE is apparently more stable among the others, losing 1 wt% up to

100 °C and 3 wt% up to 200 °C while the weight loss of other PGBNs is approximately 10 wt% at this stage. In order to rationalize the properties of the networks on a structural basis, it is necessary to identify variable network parameters as shown in Scheme 2. Essential to the structure are repeat glycidyl units with network points arising from glycerol (in GGE) and linear sections derived from monoglycidyl ethers. The two variable components in this study are the network chain segment length and the nature of monoglycidyl ether side chains. The swelling test results from Table 2, shown graphically in Fig. 3B, clearly indicate that the network chain segment length is controllable by adjusting the mole fraction of the GGE crosslinker; naturally, the monoglycidyl ether side chains are variable by the choice of monomer.

Young's moduli, determined by tensile testing, were found to be highly dependent on the crosslink density and less sensitive to the actual nature of the glycidyl ether side chains incorporated. As seen in Fig. 5A, an almost linear dependence can be drawn between the mole fraction of GGE crosslinker and the modulus value. It is not possible to conclude any significant difference between the copolymer network series of differing sidechains,
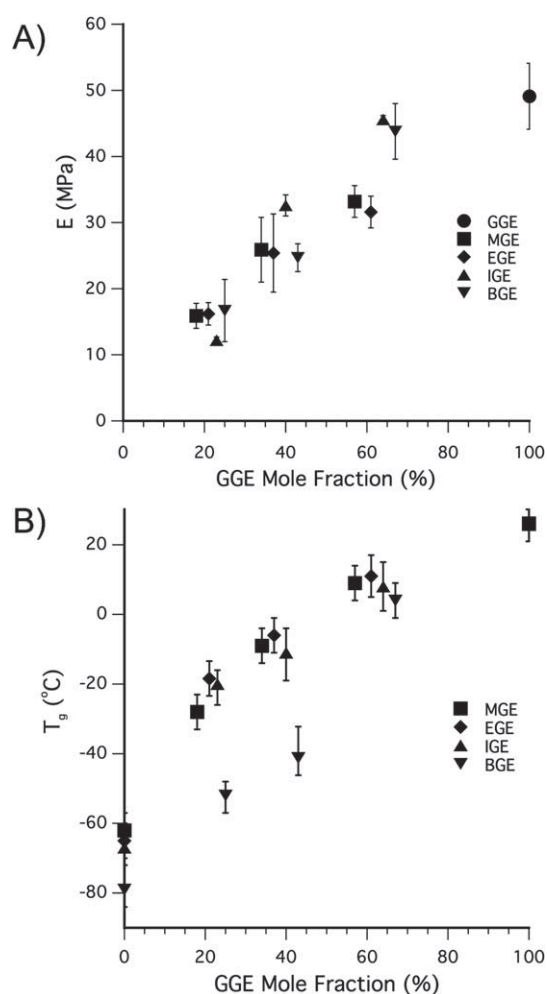

Fig. 5 Structure–property relationship between mole fraction of GGE crosslinker and (A) elastic modulus (E); (B) glass transition temperature (T_g), for the studied PGBNs; error bars indicate onset and offset of glass transition.

21106 | *J. Mater. Chem.*, 2012, **22**, 21100–21109

This journal is © The Royal Society of Chemistry 2012

suggesting that their influence is minimal for the studied networks, and that mechanical properties are dependent on the network chain segment length. For these densely crosslinked networks, the modulus is relatively high in the 10–50 MPa range and elongation at break is moderate (<10%). Work is ongoing to further increase swelling ratios and lower the material stiffness, which may be a requirement for biomaterial applications such as for substrata for adherent cells;[41] the presented data however focuses on detailed structural analyses of highly crosslinked networks. Mechanical properties are displayed in Table 4 and clear structure–property correlations can be made and are consistent throughout the series, indicating a high degree of homogeneity.

As determined by DSC, the glass transition temperature is also proportional to crosslink density of the networks as shown in Fig. 5B. As a clear trend, T_g increases as the mole fraction of the incorporated GGE crosslinker is increased, which is typical for polymer network structures.[42] Pure GGE when polymerized has a T_g of 26 °C with copolymers having lower T_g, which varies between this maximum and the corresponding minimum T_g of the respective monoglycidyl ether homopolymers (values in Table 4).[43] This variance in T_g correlates to the ratio of monoglycidyl ether to crosslinker GGE and is also specific to the nature of the monoglycidyl ether sidechain. For example, it is evident in Fig. 5B that replacing MGE with BGE in the copolymer network leads to a significant drop in T_g across the range of copolymer ratios, which is consistent with T_g values of the homopolymers polyMGE (−62 °C) and polyBGE (−79 °C). This phenomenon can be attributed to the increased mobility of longer alkyl side chains, although this can be complicated by free volume effects and would merit a separate study.[44] It is noteworthy that despite the highly crosslinked architecture, these polymer networks are above the T_g at around room temperature or physiological temperature. These results indicate a polymer network system in which mechanical and thermal properties are dependent on the crosslink density, whilst alkyl sidechains incorporated in linear segments exert a significant influence on the overall thermal properties.

In order to gain more detailed information on the scale of molecular processes occurring during thermal transition, DMTA measurements were conducted, measuring storage and loss moduli over a temperature range. The results of DMTA measurements are shown in Fig. 6. As the glass transition is approached loss modulus E'' rises to a maximum consistent with increased mobility of the polymer chains in the network. For the studied PGBNs the temperature values at the maximum of loss modulus are consistent with the glass transition temperature values obtained from DSC. As the material becomes deformable with increasing temperature, storage modulus E' decreases. The rise in E'' concomitant with lowering of storage modulus E' leads to an increase in E''/E', whose value is known as the loss factor, or tan δ. The height and shape of tan δ give information on the molecular processes occurring during the thermal transition, and the position of the highest point relates to the glass transition temperature.[45] For the studied networks, tan δ is generally observed as a single relatively narrow peak indicating that molecular relaxations occur in a narrow range of temperatures and a single transition occurs. This is a strong support for a highly homogeneous network.[46]

The intensity of the tan δ peak is high (often >1) for the measured materials, which indicates good damping properties, particularly with networks containing higher fractions of the chain extender.[47] This is due to the density of kinetic units, which become mobile during the transition from the glassy to the rubbery state (tan δ can be interpreted as the ratio of viscous to elastic components of a system).[46] This phenomenon may be inherent to the network backbone but also most likely has significant contributions from the glycidyl ether sidechains. This large increase in kinetic mobility around the glass transition is an interesting characteristic and in preliminary studies allows for shape-memory effects and thermally controlled diffusion through the networks. In certain cases of copolymers with IGE and BGE ($G_{60}I_{40}$, $G_{80}I_{20}$ and $G_{60}B_{40}$, $G_{80}B_{20}$ in Fig. 6G and H respectively) significant shoulders to the tan δ peak were observed. This could indicate two separate thermal transitions occurring during the switch to the rubbery state, and would

Table 4 Mechanical properties of PGBNs determined by tensile tests at room temperature; Young's modulus (E), tensile strength at yield point (σ_y), elongation at yield point (ε_y), tensile strength at break (σ_B), elongation at break (ε_B)

Series	T_g, DSC [°C]	E [MPa]	σ_y [MPa]	ε_y [%]	σ_B [MPa]	ε_B [%]
G_{100}	26	49.1 ± 0.5	2.2 ± 0.5	4.7 ± 1.4	2.2 ± 0.5	4.7 ± 1.4
$G_{80}M_{20}$	−7	33.2 ± 2.4	4.2 ± 0.4	13 ± 0.7	4.0 ± 0.5	13 ± 0.7
$G_{60}M_{40}$	−9	25.9 ± 4.9	1.4 ± 0.6	6.2 ± 2.3	1.4 ± 0.6	6.2 ± 3.0
$G_{40}M_{60}$	−28	15.9 ± 1.9	1.3 ± 0.2	10 ± 1.6	1.3 ± 0.2	10 ± 1.7
M_{100}	−62					
$G_{80}E_{20}$	17	31.6 ± 2.4	3.5 ± 1.0	12 ± 3.1	3.3 ± 1.1	12 ± 3.1
$G_{60}E_{40}$	−40	25.4 ± 5.9	2.6 ± 0.3	4.5 ± 0.3	2.2 ± 0.2	4.6 ± 0.3
$G_{40}E_{60}$	−41	16.2 ± 1.7	0.6 ± 0.5	3.7 ± 0.5	0.6 ± 0.6	3.7 ± 0.5
E_{100}	−65					
$G_{80}I_{20}$	14	45.6 ± 0.6	3.1 ± 0.3	7.4 ± 0.7	2.7 ± 0.4	7.5 ± 0.7
$G_{60}I_{40}$	−11	32.6 ± 1.6	1.4 ± 0.4	4.6 ± 1.4	1.2 ± 0.4	4.6 ± 1.3
$G_{40}I_{60}$	−20	12.2 ± 0.5	0.5 ± 0.1	4.9 ± 0.5	0.4 ± 0.1	5.0 ± 0.5
I_{100}	−67					
$G_{80}B_{20}$	4	43.8 ± 4.2	2.4 ± 0.5	6.0 ± 1.3	2.2 ± 0.6	6.1 ± 1.2
$G_{60}B_{40}$	−41	24.7 ± 2.1	0.8 ± 0.1	3.6 ± 0.6	0.8 ± 0.1	3.7 ± 0.6
$G_{40}B_{60}$	−52	16.7 ± 4.7	0.3 ± 0.3	2.2 ± 1.7	0.3 ± 0.3	2.2 ± 1.7
B_{100}	−79					

This journal is © The Royal Society of Chemistry 2012

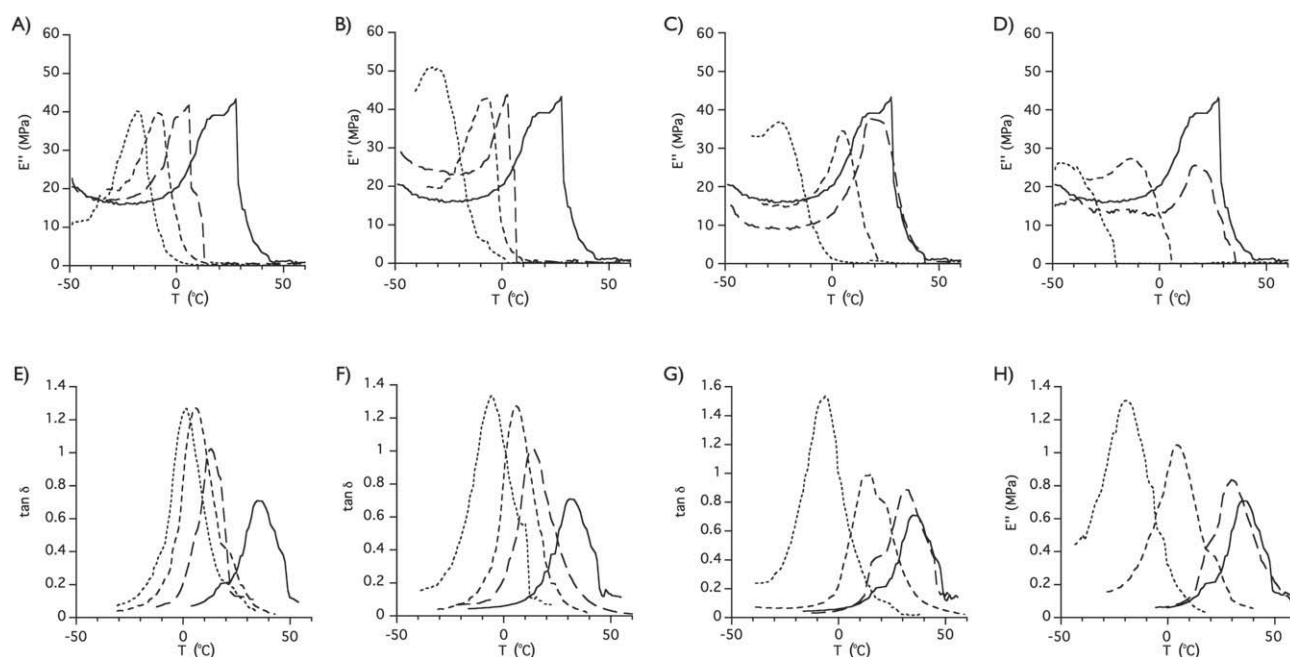*J. Mater. Chem.*, 2012, **22**, 21100–21109 | 21107

Fig. 6 Dynamic mechanical characterization at varied temperature (DMTA) of studied networks: loss modulus E'' (A–D); tan δ (E–H), for MGE, EGE, IGE and BGE incorporated networks respectively, with 0 (—), 20 (— —), 40 (---), 60 (▪ ▪ ▪ ▪ ▪) wt% of alkyl glycidyl ether incorporated for each series (sample nomenclature shown in Table 1).

signify some heterogeneity in the structure.[48] Alternatively it could arise from beta transitions corresponding to thermal relaxation of the glycidyl ether isopropyl or butyl side chains (as for example with poly(*N*-isopropylacrylamide)); as such, side chain variation could provide a useful tool for tuning thermoresponsive properties in PGBNs.[49]

Conclusions

The data presented herein give a detailed characterization of bulk, highly branched polyether networks, investigating their structural, thermal, and mechanical properties. The prepared films are highly translucent, which indicates an amorphous structure and is a desirable property for applications such as microscopic imaging, if such materials were used as substrates for cell adhesion. Each sample exhibits a single thermal glass transition below room temperature. Mechanical properties can be tuned by varying the crosslink density through incorporation of monoglycidyl ethers. This piece of evidence points towards glycidyl ether side chains having significant influences on thermal transitions within the network, which could be exploited for design of smart materials. By varying the comonomer ratio it is possible to control the network chain segment length which has a very clear influence on network behavior such as swelling, and on the mechanical properties. These findings are all characteristic of a homogeneous network structure, which can be modified towards a range of desired properties due to the defined structure–property relationships identified in this study. Investigations on cytocompatibility, protein resistance and hemocompatibility of such materials are ongoing and will be reported in future. As is the case with dendritic polyglycerols, it is anticipated that these materials could serve as analogues to the

polyethylene glycol based biomaterials. Although PEG based materials are well established, the polyglycerol architecture differs by having chemical homogeneity throughout the network as branching is inherent to the system (compared to linear PEG which requires functionalization). Also, due to the highly branched nature of the polymer multiple endgroups are available for functionalization of the polymer surface. The adjustability of their mechanical properties as well as the option to couple bioactive molecules to the material surface makes these materials promising candidate materials for regenerative therapies, where multifunctionality is highly valued to temporarily substitute organ/tissue functions and at the same time induce endogenous regeneration processes.

Notes and references

1 N. A. Peppas, J. Z. Hilt, A. Khademhosseini and R. Langer, *Adv. Mater.*, 2006, **18**, 1345.
2 B. V. Slaughter, S. S. Khurshid, O. Z. Fisher, A. Khademhosseini and N. A. Peppas, *Adv. Mater.*, 2009, **21**, 3307.
3 M. S. Shoichet, *Macromolecules*, 2010, **43**, 581.
4 K. Knop, R. Hoogenboom, D. Fischer and U. S. Schubert, *Angew. Chem., Int. Ed.*, 2010, **49**, 6288.
5 S. Drotleff, U. Lungwitz, M. Breunig, A. Dennis, T. Blunk, J. Tessmar and A. Gopferich, *Eur. J. Pharm. Biopharm.*, 2004, **58**, 385.
6 J. M. Zhu, *Biomaterials*, 2010, **31**, 4639.
7 R. K. Kainthan, S. R. Hester, E. Levin, D. V. Devine and D. E. Brooks, *Biomaterials*, 2007, **28**, 4581.
8 D. Wilms, S. E. Stiriba and H. Frey, *Acc. Chem. Res.*, 2010, **43**, 129.
9 M. A. R. Meier, J. O. Metzger and U. S. Schubert, *Chem. Soc. Rev.*, 2007, **36**, 1788.
10 A. L. Sisson and R. Haag, *Soft Matter*, 2010, **6**, 4968.
11 D. Steinhilber, S. Seiffert, J. A. Heyman, F. Paulus, D. A. Weitz and R. Haag, *Biomaterials*, 2011, **32**, 1311.
12 E. A. T. Vargas, N. C. D. Baracho, J. de Brito and A. A. A. de Queiroz, *Acta Biomater.*, 2010, **6**, 1069.

21108 | *J. Mater. Chem.*, 2012, **22**, 21100–21109

This journal is © The Royal Society of Chemistry 2012

13 N. E. Fedorovich, M. H. Oudshoorn, D. van Geemen, W. E. Hennink, J. Alblas and W. J. A. Dhert, *Biomaterials*, 2009, **30**, 344.

14 M. Weinhart, T. Becherer and R. Haag, *Chem. Commun.*, 2011, **47**, 1553.

15 A. Sunder, R. Hanselmann, H. Frey and R. Mulhaupt, *Macromolecules*, 1999, **32**, 4240.

16 E. J. Vandenberg, *J. Polym. Sci., Polym. Chem. Ed.*, 1985, **23**, 915.

17 R. K. Kainthan, E. B. Muliawan, S. G. Hatzikiriakos and D. E. Brooks, *Macromolecules*, 2006, **39**, 7708.

18 M. H. M. Oudshoorn, R. Penterman, R. Rissmann, J. A. Bouwstra, D. J. Broer and W. E. Hennink, *Langmuir*, 2007, **23**, 11819.

19 M. H. M. Oudshoorn, R. Rissmann, J. A. Bouwstra and W. E. Hennink, *Biomaterials*, 2006, **27**, 5471.

20 A. Dworak, W. Walach and B. Trzebicka, *Macromol. Chem. Phys.*, 1995, **196**, 1963.

21 R. Tokar, P. Kubisa, S. Penczek and A. Dworak, *Macromolecules*, 1994, **27**, 320.

22 A. L. Sisson, D. Steinhilber, T. Rossow, P. Welker, K. Licha and R. Haag, *Angew. Chem., Int. Ed.*, 2009, **48**, 7540.

23 H. X. Zhou, D. Steinhilber, H. Schlaad, A. L. Sisson and R. Haag, *React. Funct. Polym.*, 2011, **71**, 356.

24 J. V. Crivello, *J. Polym. Sci., Part A: Polym. Chem.*, 2006, **44**, 6435.

25 J. V. Crivello, *J. Polym. Sci., Part A: Polym. Chem.*, 2006, **44**, 3036.

26 S. F. Chen, L. Y. Li, C. Zhao and J. Zheng, *Polymer*, 2010, **51**, 5283.

27 P. D. Drumheller and J. A. Hubbell, *Anal. Biochem.*, 1994, **222**, 380.

28 D. G. Castner and B. D. Ratner, *Surf. Sci.*, 2002, **500**, 28.

29 V. P. Shastri and A. Lendlein, *MRS Bull.*, 2010, **35**, 571.

30 D. Rana and T. Matsuura, *Chem. Rev.*, 2010, **110**, 2448.

31 S. J. Todd, D. Farrar, J. E. Gough and R. V. Ulijn, *Soft Matter*, 2007, **3**, 547.

32 S. J. Todd, D. J. Scurr, J. E. Gough, M. R. Alexander and R. V. Ulijn, *Langmuir*, 2009, **25**, 7533.

33 B. C. Kallukalam, M. Jayabalan and V. Sankar, *Biomed. Mater.*, 2009, **4**, 015002.

34 E. Diez, G. Ovejero, M. D. Romero, I. Diaz and S. Bertholdy, *Chem. Eng. Trans.*, 2011, **24**, 553.

35 J. V. Crivello, *J. Polym. Sci., Part A: Polym. Chem.*, 2009, **47**, 866.

36 J. L. Dektar and N. P. Hacker, *J. Org. Chem.*, 1990, **55**, 639.

37 P. Chiniwalla, Y. Q. Bai, E. Elce, R. Shick, W. C. McDougall, S. A. B. Allen and P. A. Kohl, *J. Appl. Polym. Sci.*, 2003, **89**, 568.

38 H. M. Badawi and S. A. Ali, *Spectrochim. Acta, Part A*, 2009, **74**, 558.

39 J. V. Crivello and J. H. W. Lam, *J. Polym. Sci., Polym. Chem. Ed.*, 1978, **16**, 2441.

40 K. M. Dean, W. D. Cook and M. Y. Lin, *Eur. Polym. J.*, 2006, **42**, 2872.

41 R. A. Marklein and J. A. Burdick, *Soft Matter*, 2010, **6**, 136.

42 A. Lendlein, J. Zotzmann, Y. K. Feng, A. Alteheld and S. Kelch, *Biomacromolecules*, 2009, **10**, 975.

43 Y. Hirose and K. Adachi, *Macromolecules*, 2006, **39**, 1779.

44 L. Kwisnek, M. Kaushik, C. E. Hoyle and S. Nazarenko, *Macromolecules*, 2010, **43**, 3859.

45 S. Kelch, N. Y. Choi, Z. G. Wang and A. Lendlein, *Adv. Eng. Mater.*, 2008, **10**, 494.

46 H. Ishida and D. J. Allen, *Polymer*, 1996, **37**, 4487.

47 D. S. Jones, *Int. J. Pharm.*, 1999, **179**, 167.

48 X. X. Jian, L. Q. Xiao, W. L. Zhou and F. M. Xu, *Polym. Bull.*, 2009, **63**, 225.

49 J. F. Lutz, O. Akdemir and A. Hoth, *J. Am. Chem. Soc.*, 2006, **128**, 13046.

This journal is © The Royal Society of Chemistry 2012

J. Mater. Chem., 2012, **22**, 21100–21109 | 21109